Journal of Engg. Research **Vol. 5 No. (6) March 2018 pp.** *1-14*

التحكم في الارتفاع الفوضوي لمركبة فضائية مع فشل بعض الحساسات على أساس وضع الانزلاق المتكامل

تشوانغ ليو*، كيكي شي و زاوي سون
مركز بحوث تكنولوجيا الأقمار الصناعية، معهد هاربين للتكنولوجيا، هاربين 150001، الصين
* مراسلة المؤلف: liuchuangforever@msn.com

الخلاصة

تبحث هذه الورقة في مشكلة الموقف الفوضوي للمركبة الفضائية مع الفشل في بعض المحرك والتحكم في المدخل. أولا، نظام المركبة الفضائية الفوضى مكتوب في شكل معادلة غير خطية تحت تأثير ثلاثة مدخلات.

عند فشل محرك أو اثنان، يمكن تكوين معادلة غير خطية تحت تأثير مدخل واحد أو مدخلين.

لتلبية متطلبات المهمة، يتم تنفيذ تخطيط المسار مقدما، ويمكن الحصول على معادلة ديناميكية من خطأ سرعة الزاوية. ثم، يتم دمج أفكار التحكم في الانزلاق متكاملة في وحدة تحكم، والذي يتكون من السيطرة إنهاء وإنهاء السيطرة. وأخيرا، يتم إجراء عمليات المحاكاة لتقييم أداء وحدة التحكم المقترحة. وتشير نتائج المحاكاة إلى أن وحدة التحكم لها الخصائص التالية: (أ) القضاء على حركة الموقف الفوضوية؛ (ب) النظر الصريح في القيود المفروضة على مدخلات التحكم؛ (ج) افتراض الموقف الزمني لتحقيق الاستقرار؛ (د) تتبع مسار السرعة الزاوية المرجعية المصممة في السابق (هـ) النظر في فشل مشغل معين، (و) المتانة لعزم دوران اضطراب خارجي أكبر.

Spacecraft chaotic attitude control with certain actuator failure based on integral sliding mode

Chuang Liu*, Keke Shi and Zhaowei Sun

Research Center of Satellite Technology, Harbin Institute of Technology, Harbin 150001, China

**Corresponding Author: liuchuangforever@msn.com*

ABSTRACT

This paper investigates the control problem of spacecraft chaotic attitude motion with certain actuator failure and control input constraint. First, the spacecraft chaotic attitude system is written in a nonlinear equation form of three inputs. When the failure of one actuator or failures of two actuators exist, it can be transformed into a nonlinear equation form of double input or single input, respectively. To satisfy task-requirement, trajectory planning is performed in advance, and the dynamics equation of angular velocity error can be obtained. Then, integral sliding mode ideas are incorporated into the controller, which consists of equivalent control term and switching control term. Finally, simulations are performed to assess the performance of the proposed controller. The simulation results indicate that the controller has the following characteristics: (a) elimination of chaotic attitude motion, (b) explicit consideration of control input constraint, (c) presupposition of attitude stabilization time, (d) track reference angular velocity trajectory designed in advance, (e) consideration of certain actuator failure, and (f) robustness to bigger external disturbance torque.

Keywords: Attitude system; actuator failure; chaotic motion; integral sliding mode; linear matrix inequality.

INTRODUCTION

As space technologies have developed and progressed, advanced space missions have put forward higher requirements for spacecraft attitude control system to ensure rapid and accurate response in the presense of certain actuator failure, control input constraint, and external disturbances. A significant challege arises when these issues are considered simultaneously. Particularly, the external disturbances often constituted of periodic and secular term; once the spacecraft properties and external disturbances imposed on it satisfy a certain condition, it can lead to chaotic attitude motion, which will cause great damage in the spacecraft. Consequently, the chaotic attitude control with certain actuator failure is extremely important in the space mission.

Many flight experiences across the world's aerospace history have witnessed the spacecraft attitude motion with unexpected behaviors, which results from the external disturbances that had not been taken into consideration in the process of spacecraft design. Numerous theoretical researches have pointed out that spacecraft chaotic motion exists under the influence of different external disturbances (Beletsky *et al.*, 1999; Meehan & Asokanthan, 2002; Aghababa & Aghababa, 2013). Chen system (Lu & Chen, 2006) and Lu system (Lu, 2006) are two typical chaotic systems that the spacecraft attitude system may become. Classical chaotic control methods include adaptive control (Wei, 2015), sliding mode control (Ke *et al.*, 2015), fuzzy logic control (Yau & Shieh, 2008), and linear matrix inequality technique (Kuntanapreeda, 2009). In recent years,

considerable efforts have been made to study the attitude stabilization control and fault-tolerant control of spacecraft during rotational maneuvers, and the theory of controller design has been developed in a variety of directions (Zhang & Jiang, 2008; Zolghadri, 2012; Zhang *et al.*, 2014). The frequently used methods include H∞ control (Yang *et al.*, 2001; Luo *et al.*, 2005), adaptive control (Ma *et al.*, 2015), feedback linearization (Wang & Wu, 2015), sliding mode control (Alwi *et al.*, 2008), and linear matrix inequality technique (Liao *et al.*, 2002). Among them, the sliding mode control strategy is acknowledged as an effective way to withstand the actuator failure and external disturbances, which has been widely used in aircraft or spacecraft attitude control systems. In the study of Alwi & Edwards (2008), a fault-tolerant sliding mode control scheme was proposed for the aircraft operating phase with an actuator failure, where it allowed control allocation. According to Xiao *et al.* (2012), an adaptive fault-tolerant sliding mode control scheme was developed for attitude tracking of flexible spacecraft with partial loss of actuator effectiveness, where neural networks were introduced to cope with system uncertainties, and online updating law was developed to estimate actuator failure bound. In the paper of Hu (2012), an adaptive sliding mode control scheme with L2 gain performance has been evaluated to perform attitude tracking control for flexible spacecraft with actuator failures, parameter uncertainties, and external disturbances. Utkin *et al.* (2009) pointed out that the system dynamics might be fragile to failures during the reaching phase. To cope with this problem, the idea of integral sliding mode control was presented (Utkin & Shi, 1996; Rubagotti *et al.*, 2011). This can ensure that the sliding surface begins from the initial time instant, which eliminates the reaching phase (Shen *et al.*, 2015).

The main stabilization results for the case when certain actuator failures occur to the spacecraft have been presented in some literature. According to Crouch (1984), sufficient and necessary conditions for the controllability of rigid spacecraft in the case of one, two, and three independent control torques were provided. He pointed out that controllability was impossible with fewer than three devices in the case of momentum exchange devices. Additionally, Kerai (1995) pointed out that the rigid body system was never small-time locally controllable with only one control. The angular velocity equations can be made asymptotically stable about the origin by means of two control torques along the principal axes (Brockett, 1983). Aeyels (1985) used one torque alligned with a principal axis to investigate the feedback stabilization problem of the zero solution of angular velocity equations. However, it is required that the moment of inertia of the rigid body along that principal axis should be the largest or the smallest. Bloch & Marsden (1990) also validated this conclusion. Aeyels & Szafranski (1988) also showed that a single control aligned with a principal axis cannot stabilize the rigid body system. We believe that, under given conditions, the spacecraft chaotic attitude system will be controllable when the failures of two actuators occur.

Motivated by the above researches, an integral sliding mode-based control strategy is developed for the spacecraft chaotic attitude motion with certain actuator failure and control input constraint, where the linear matrix inequality technique is incorporated into the controller design. Also, the potential effects of external disturbances on system performance are explicitly investigated during the attitude dynamics and problem statement process. Compared with most existing spacecraft attitude control approaches, the presented control scheme only requires a quantitative relation of the moment of inertia without precise information, and the fault detection mechanism is not required to detect the actuator failure. Furthermore, the proposed control law could track the attitude motion

trajectory designed in advance and use the linear matrix inequality technique to obtain the unknown matrices introduced in the integral sliding mode. Using the Lyapunov method, the stability analysis of the resulting closed-loop system is demonstrated in detail, and the effectiveness of the proposed control method is also analyzed via numerical simulations.

The remainder of this paper is organized as follows. The next section introduces the spacecraft attitude dynamics equation and writes it in a nonlinear equation form of three inputs. Besides, this section describes two kinds of chaos phenomenon in the spacecraft attitude motion influenced by external disturbances and transforms the nonlinear equation form of three inputs into that of double input and single input under the condition of actuator failures. Then, the purpose of this work is addressed, followed by the section that presents the integral sliding mode-based robust controller. Numerical simulations are performed to illustrate the performance of the controller. Finally, the conclusions of this work are drawn.

ATTITUDE DYNAMICS AND PROBLEM STATEMENT

Supposing the spacecraft is a rigid body with actuators that provide control torques with regard to three mutually perpendicular axes that define a body reference frame. The attitude dynamics equation is given by

$$\boldsymbol{I}\dot{\boldsymbol{\omega}} + \boldsymbol{\omega} \times (\boldsymbol{I}\boldsymbol{\omega}) = \boldsymbol{T}_c + \boldsymbol{T}_d \tag{1}$$

where $\boldsymbol{\omega} = \begin{bmatrix} \omega_1 & \omega_2 & \omega_3 \end{bmatrix}^{\mathrm{T}}$ means the angular velocity of the body reference frame with respect to the earth-centered inertial reference frame represented in the body reference frame, $\boldsymbol{I}$ denotes the spacecraft inertia matrix, $\boldsymbol{T}_c$ represents the control input torque, and $\boldsymbol{T}_d$ means the external disturbance torque imposed on the spacecraft, which is generally expressed in the following nonlinear form:

$$\boldsymbol{T}_d = \boldsymbol{D}\boldsymbol{\omega} + \boldsymbol{M} \tag{2}$$

where $\boldsymbol{D} = \left[d_{ij} \right]_{3\times 3} \in \boldsymbol{R}^{3\times 3} (i, j = 1, 2, 3)$, which can be a constant matrix or matrix varying with angular velocity; $\boldsymbol{M} = \left[m_i \right]_{3\times 1} \in \boldsymbol{R}^{3\times 1} (i = 1, 2, 3)$, which can be a constant matrix or matrix varying with angular velocity, or even periodic matrix or long-term matrix. Use Levi-Civita symbol in three dimensions to express vector products, denoted as ε_{kij}, and the corresponding definition is as follows:

$$\varepsilon_{kij} = \begin{cases} +1, if\ (k,i,j)\ is\ (1,2,3),(2,3,1)\ or\ (3,1,2) \\ -1, if\ (k,i,j)\ is\ (3,2,1),(1,3,2)\ or\ (2,1,3) \\ 0,\ if\ i = j\ or\ j = k\ or\ k = i \end{cases} \tag{3}$$

For any two vectors $\boldsymbol{p} = [p_i]_{3\times 1} (i = 1, 2, 3), \boldsymbol{q} = [q_j]_{3\times 1} (j = 1, 2, 3)$, we have $\sum_{i,j} \varepsilon_{kij} p_i q_j = (\boldsymbol{p} \times \boldsymbol{q})_k$, where $()_k$ represents the k-th component of the vector product.

Combining equation (1) and equation (2), and writing in the component form, we have

$$\begin{cases} I_1\dot{\omega}_1 - (I_2 - I_3)\omega_2\omega_3 = T_{c1} + d_{11}\omega_1 + d_{12}\omega_2 + d_{13}\omega_3 + m_1 \\ I_2\dot{\omega}_2 - (I_3 - I_1)\omega_1\omega_3 = T_{c2} + d_{21}\omega_1 + d_{22}\omega_2 + d_{23}\omega_3 + m_2 \\ I_3\dot{\omega}_3 - (I_1 - I_2)\omega_1\omega_2 = T_{c3} + d_{31}\omega_1 + d_{32}\omega_2 + d_{33}\omega_3 + m_3 \end{cases} \tag{4}$$

where I_1, I_2 and I_3 denote the three components of inertia matrix; T_{c1}, T_{c2} and T_{c3} denote the three components of control input torque.

Then,

$$\begin{cases} \dot{\omega}_1 = I_1^{-1}(I_2 - I_3)\omega_2\omega_3 + I_1^{-1}d_{11}\omega_1 + I_1^{-1}d_{12}\omega_2 + I_1^{-1}d_{13}\omega_3 + I_1^{-1}T_{c1} + I_1^{-1}m_1 \\ \dot{\omega}_2 = I_2^{-1}(I_3 - I_1)\omega_1\omega_3 + I_2^{-1}d_{21}\omega_1 + I_2^{-1}d_{22}\omega_2 + I_2^{-1}d_{23}\omega_3 + I_2^{-1}T_{c2} + I_2^{-1}m_2 \\ \dot{\omega}_3 = I_3^{-1}(I_1 - I_2)\omega_1\omega_2 + I_3^{-1}d_{31}\omega_1 + I_3^{-1}d_{32}\omega_2 + I_3^{-1}d_{33}\omega_3 + I_3^{-1}T_{c3} + I_3^{-1}m_3 \end{cases} \tag{5}$$

Let

$$\boldsymbol{B} = \begin{bmatrix} I_1^{-1}d_{11} & I_1^{-1}d_{12} & I_1^{-1}d_{13} \\ I_2^{-1}d_{21} & I_2^{-1}d_{22} & I_2^{-1}d_{22} \\ I_3^{-1}d_{31} & I_3^{-1}d_{32} & I_3^{-1}d_{33} \end{bmatrix}, f(\boldsymbol{\omega}) = \boldsymbol{A}\begin{bmatrix} \omega_2\omega_3 \\ \omega_1\omega_3 \\ \omega_1\omega_2 \end{bmatrix} + \hat{\boldsymbol{C}},$$

$$\boldsymbol{A} = \mathrm{diag}(I_1^{-1}(I_2 - I_3), I_2^{-1}(I_3 - I_1), I_3^{-1}(I_1 - I_2)),$$

$$\hat{\boldsymbol{C}} = \begin{bmatrix} I_1^{-1}m_1 & I_2^{-1}m_2 & I_3^{-1}m_3 \end{bmatrix}^{\mathrm{T}}, \boldsymbol{u} = \begin{bmatrix} I_1^{-1}T_{c1} & I_2^{-1}T_{c2} & I_3^{-1}T_{c3} \end{bmatrix}^{\mathrm{T}}$$

Then, equation (5) can be transformed into the following form:

$$\dot{\boldsymbol{\omega}} = \boldsymbol{B}\boldsymbol{\omega} + f(\boldsymbol{\omega}) + \boldsymbol{u} \tag{6}$$

First, two examples of the spacecraft attitude motion are analyzed when the control torques that actuators provide are zero, namely, when u=0.

Example 1: When the moment of inertia and the external disturbances acted on the spacecraft satisfy

$$I_1 = 2I_2 = 2I_3$$

$$\boldsymbol{T}_d = \begin{bmatrix} I_1 a(\omega_2 - \omega_1) \\ I_2(c\omega_1 - a\omega_1 + c\omega_2) \\ -I_3 b\omega_3 \end{bmatrix}$$

Equation (5) is transformed into the Chen system form,

$$\begin{cases} \dot{\omega}_1 = a(\omega_2 - \omega_1) \\ \dot{\omega}_2 = (c - a)\omega_1 + c\omega_2 - \omega_1\omega_3 \\ \dot{\omega}_3 = \omega_1\omega_2 - b\omega_3 \end{cases} \tag{7}$$

When $a = 35, b = 3, c = 28$, the system denoted by equation (7) is a chaotic system, and the chaotic attractor and its projection are shown in Fig.1, from which we can obviously see that the spacecraft attitude motion is chaotic.

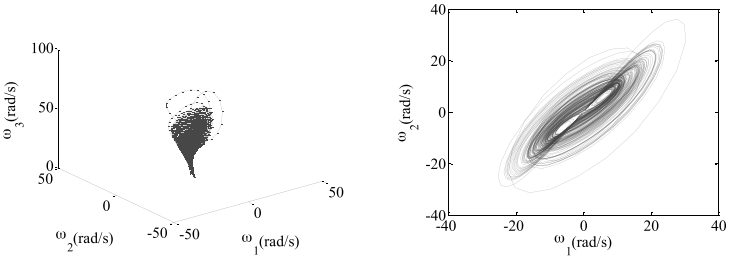

(a) ω_1-ω_2-ω_3 3D graph (b) ω_1-ω_2 plane projection

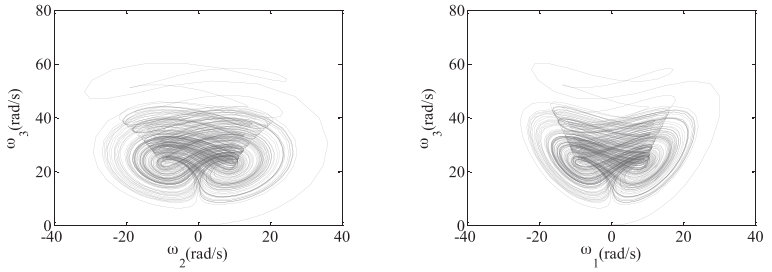

(c) ω_2-ω_3 plane projection (d) ω_1-ω_3 plane projection

Figure 1. Spacecraft attitude Chen system chaotic attractor and its projection.

Example2: When the moment of inertia and the external disturbances acted on the spacecraft satisfy

$$I_1 = 2I_2 = 2I_3$$

$$\boldsymbol{T}_d = \begin{bmatrix} I_1 a(\omega_2 - \omega_1) \\ I_2 c\omega_2 \\ -I_3 b\omega_3 \end{bmatrix}$$

Equation (5) is transformed into the Lu system form,

$$\begin{cases} \dot{\omega}_1 = a(\omega_2 - \omega_1) \\ \dot{\omega}_2 = c\omega_2 - \omega_1\omega_3 \\ \dot{\omega}_3 = \omega_1\omega_2 - b\omega_3 \end{cases} \tag{8}$$

When $a = 36, b = 3, c = 20$, the system denoted by equation (8) is a chaotic system, and the chaotic attractor and its projection are shown in Fig.2, from which we can also see that the spacecraft attitude motion is chaotic.

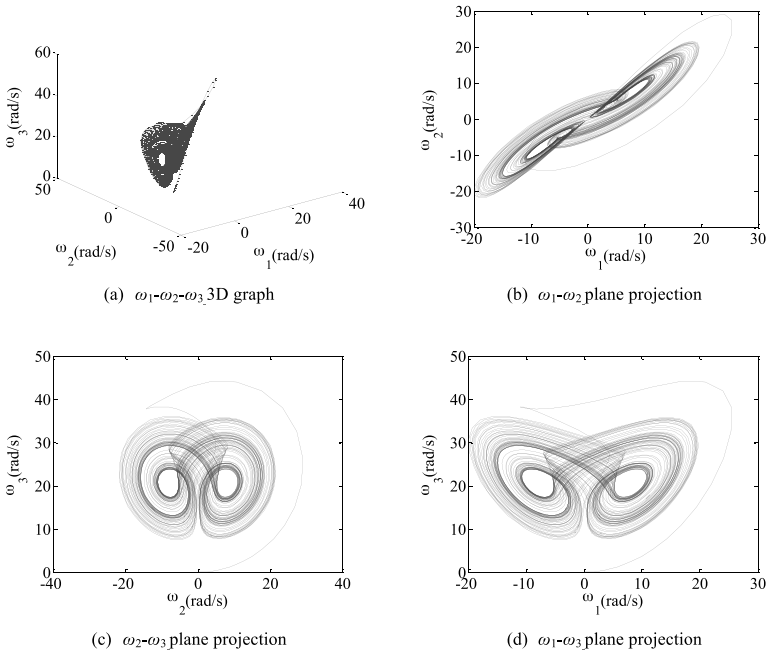

(a) ω_1-ω_2-ω_3 3D graph (b) ω_1-ω_2 plane projection

(c) ω_2-ω_3 plane projection (d) ω_1-ω_3 plane projection

Figure 2. Spacecraft attitude Lu system chaotic attractor and its projection.

Under the condition of total fault or failure of certain actuators, the sliding mode controller can be designed. Two cases are considered, that is, the failure of one actuator and failures of two actuators.

Case 1 (failure of one actuator): Two control inputs are added into the system; take the failure of actuator installed on the x-axis for example.

In this case, we have $T_{c1}=0$. The attitude dynamics system denoted by equation (6) can be transformed into the following nonlinear equation of double input:

$$\dot{\boldsymbol{\omega}}=\boldsymbol{B}\boldsymbol{\omega}+f(\boldsymbol{\omega})+\begin{bmatrix}0\\u_2\\u_3\end{bmatrix}=\boldsymbol{B}\boldsymbol{\omega}+f(\boldsymbol{\omega})+\begin{bmatrix}0&0\\1&0\\0&1\end{bmatrix}\begin{bmatrix}u_2\\u_3\end{bmatrix}=\boldsymbol{B}\boldsymbol{\omega}+f(\boldsymbol{\omega})+\boldsymbol{F}\boldsymbol{u}^* \tag{9}$$

where

$$\boldsymbol{F}=\begin{bmatrix}0&0\\1&0\\0&1\end{bmatrix},\boldsymbol{u}^*=\begin{bmatrix}u_2\\u_3\end{bmatrix}$$

Case 2 (failures of two actuators): Only one control input is added into the system; take the failures of actuators installed on the x-axis and y-axis for example.

In this case, we have $T_{c1}=0, T_{c2}=0$. The attitude dynamics system denoted by equation (6) can be transformed into the following nonlinear equation of single input:

$$\dot{\boldsymbol{\omega}}=\boldsymbol{B}\boldsymbol{\omega}+f(\boldsymbol{\omega})+\begin{bmatrix}0\\0\\u_3\end{bmatrix}=\boldsymbol{B}\boldsymbol{\omega}+f(\boldsymbol{\omega})+\begin{bmatrix}0\\0\\1\end{bmatrix}u_3=\boldsymbol{B}\boldsymbol{\omega}+f(\boldsymbol{\omega})+\boldsymbol{F}\boldsymbol{u}^* \tag{10}$$

where

$$\boldsymbol{F}=\begin{bmatrix}0\\0\\1\end{bmatrix},\boldsymbol{u}^*=u_3$$

Then, by analyzing equation (10) , it is obviously seen that the spacecraft chaotic attitude system can be controllable if and only if the two initial angular velocities along the x-axis and y-axis are zero, namely, $\omega_{10}=\omega_{20}=0$, which results in $\omega_1=\omega_2=0$. We just need to design u_3 to stabilize the angular velocity along the z-axis.

The purpose of this work is to design a control input $\boldsymbol{u}^*$ for the spacecraft attitude dynamics system with chaotic attitude motion and certain actuator failure, such that, for all physically possible initial conditions, all $\boldsymbol{u}\le\boldsymbol{u}_m$, all $\boldsymbol{I}=\boldsymbol{I}^{\mathrm{T}}>0$, and the following is achieved within a given finite time: $\lim\boldsymbol{\omega}=\boldsymbol{0}$.

SLIDING MODE CONTROLLER DESIGN

To meet the necessary observation mission or the requirement of control input constraint, the spacecraft angular acceleration should track a given reference trajectory. Assume that the maximum of yaw angular acceleration is $\dot{\omega}_m > 0$, and the reference trajectory of yaw angular acceleration $\dot{\omega}_{dr}$ is shown in Fig.3.

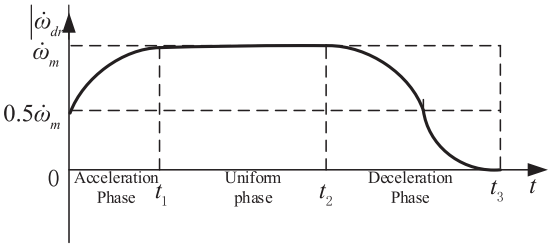

Figure 3. Reference trajectory of yaw angular acceleration.

The corresponding mathematical expression is

$$\dot{\omega}_{dr}(t)=\begin{cases} -\dfrac{\dot{\omega}_m}{2}\left[1+\sin\left(\dfrac{\pi t}{2t_1}\right)\right] & 0\le t\le t_1 \\ -\dot{\omega}_m & t_1< t\le t_2 \\ -\dfrac{\dot{\omega}_m}{2}\left[1+\cos\left(\dfrac{t-t_2}{t_3-t_2}\pi\right)\right] & t_2< t\le t_3 \\ 0 & t>t_3 \end{cases} \tag{11}$$

Then, the mathematical expression of reference angular velocity can be represented by equation (12).

$$\omega_{dr}(t)=\begin{cases} \omega_{d0}-\dfrac{\dot{\omega}_m}{2}t+\dfrac{\dot{\omega}_m t_1}{\pi}\left(\cos\dfrac{\pi t}{2t_1}-1\right) & 0\le t\le t_1 \\ \omega_{d0}-\dfrac{\dot{\omega}_m}{2}\left(1+\dfrac{2}{\pi}\right)t_1-\dot{\omega}_m\left(t-t_1\right) & t_1< t\le t_2 \\ \omega_{d0}-\dfrac{\dot{\omega}_m}{2}\left(1+\dfrac{2}{\pi}\right)t_1-\dot{\omega}_m\left(t_2-t_1\right)-\dfrac{\dot{\omega}_m}{2}\left(t-t_2\right)-\dfrac{\dot{\omega}_m(t_3-t_2)}{2\pi}\sin\dfrac{\pi(t-t_2)}{t_3-t_2} & t_2< t\le t_3 \\ 0 & t>t_3 \end{cases} \tag{12}$$

where the maximum of angular acceleration depends on the characteristic time instant $t_i, i=1,2,3$ and the initial value of angular velocity ω_{d0}.

The maximum of yaw angular acceleration is calculated as

$$\dot{\omega}_m=\frac{2\pi\omega_{d0}}{2t_1+\pi(t_2+t_3-t_1)} \tag{13}$$

Assuming the angular velocity error is $\boldsymbol{e}$, then the derivative of angular velocity error with respect to time is

$$\dot{\boldsymbol{e}}=\dot{\boldsymbol{\omega}}-\dot{\boldsymbol{\omega}}_d=\boldsymbol{B}\boldsymbol{\omega}+f(\boldsymbol{\omega})+\boldsymbol{F}\boldsymbol{u}^*-\dot{\boldsymbol{\omega}}_d \tag{14}$$

The sliding mode control law constituted of equivalent control $\boldsymbol{u}_{eq}$ and switching control $\boldsymbol{u}_{sw}$. With $\dot{\boldsymbol{s}} = 0$, the equivalent control term can be obtained; then let $\boldsymbol{u}^* = \boldsymbol{u}_{eq} + \boldsymbol{u}_{sw}$, by analyzing $\boldsymbol{s}$ and substitute $\boldsymbol{u}^*$, such that $\boldsymbol{s}\dot{\boldsymbol{s}} < 0$ is satisfied, and the switching control term can be obtained. The equivalent control term ensures that the state of angular velocity error system is maintained on the sliding surface, and the switching control term ensures that the state does not leave the sliding surface.

Design integral sliding surface

$$\boldsymbol{s} = \boldsymbol{C}\boldsymbol{e} + \boldsymbol{K}\int_0^t \boldsymbol{e}dt \tag{15}$$

The definitions of matrices $\boldsymbol{C}$ and $\mathbf{K}$ will be discussed later, then

$$\dot{\boldsymbol{s}} = \boldsymbol{C}\dot{\boldsymbol{e}} + \boldsymbol{K}\boldsymbol{e} = \boldsymbol{C}(\boldsymbol{B}\boldsymbol{\omega} + f(\boldsymbol{\omega}) + \boldsymbol{F}\boldsymbol{u}^*) - \boldsymbol{C}\dot{\boldsymbol{\omega}}_d + \boldsymbol{K}\boldsymbol{\omega} - \boldsymbol{K}\boldsymbol{\omega}_d \tag{16}$$

Let $\dot{\boldsymbol{s}} = 0$, the equivalent control term

$$\boldsymbol{u}_{eq} = -\boldsymbol{C}\boldsymbol{B}\boldsymbol{\omega} - \boldsymbol{C}\boldsymbol{f}(\boldsymbol{\omega}) + \boldsymbol{C}\dot{\boldsymbol{\omega}}_d + \boldsymbol{K}\boldsymbol{\omega}_d - \boldsymbol{K}\boldsymbol{\omega} \tag{17}$$

Substituting equation (17) into equation (14) , we have

$$\dot{\boldsymbol{e}} = \boldsymbol{B}\boldsymbol{\omega} + \boldsymbol{f}(\boldsymbol{\omega}) - \boldsymbol{F}\boldsymbol{C}\boldsymbol{B}\boldsymbol{\omega} - \boldsymbol{F}\boldsymbol{C}\boldsymbol{f}(\boldsymbol{\omega}) + \boldsymbol{F}\boldsymbol{C}\dot{\boldsymbol{\omega}}_d + \boldsymbol{F}\boldsymbol{K}\boldsymbol{\omega}_d - \boldsymbol{F}\boldsymbol{K}\boldsymbol{\omega} - \dot{\boldsymbol{\omega}}_d \tag{18}$$

In Case 1, when the failure of actuator installed on the x-axis is considered, $\boldsymbol{C} = \begin{bmatrix} c_1 & 1 & 0 \\ c_2 & 0 & 1 \end{bmatrix}$.

Then,

$$\begin{aligned} \boldsymbol{f}(\boldsymbol{\omega}) - \boldsymbol{F}\boldsymbol{C}\boldsymbol{f}(\boldsymbol{\omega}) &= \begin{bmatrix} 0 \\ -\omega_1\omega_3 \\ \omega_1\omega_2 \end{bmatrix} - \begin{bmatrix} 0 & 0 \\ 1 & 0 \\ 0 & 1 \end{bmatrix} \begin{bmatrix} c_1 & 1 & 0 \\ c_2 & 0 & 1 \end{bmatrix} \begin{bmatrix} 0 \\ -\omega_1\omega_3 \\ \omega_1\omega_2 \end{bmatrix} = \begin{bmatrix} 0 \\ -\omega_1\omega_3 \\ \omega_1\omega_2 \end{bmatrix} - \begin{bmatrix} 0 & 0 & 0 \\ c_1 & 1 & 0 \\ c_2 & 0 & 1 \end{bmatrix} \begin{bmatrix} 0 \\ -\omega_1\omega_3 \\ \omega_1\omega_2 \end{bmatrix} \\ &= \begin{bmatrix} 0 \\ -\omega_1\omega_3 \\ \omega_1\omega_2 \end{bmatrix} - \begin{bmatrix} 0 \\ -\omega_1\omega_3 \\ \omega_1\omega_2 \end{bmatrix} = \mathbf{0} \end{aligned} \tag{19}$$

In Case 2, when the failures of actuators installed on the x-axis and y-axis are considered, $\omega_1 = \omega_2 = 0, \boldsymbol{C} = \begin{bmatrix} c & 0 & 1 \end{bmatrix}$.

Then,

$$\boldsymbol{f}(\boldsymbol{\omega}) - \boldsymbol{F}\boldsymbol{C}\boldsymbol{f}(\boldsymbol{\omega}) = \begin{bmatrix} 0 \\ -\omega_1\omega_3 \\ \omega_1\omega_2 \end{bmatrix} - \begin{bmatrix} 0 \\ 0 \\ 1 \end{bmatrix} \begin{bmatrix} c & 0 & 1 \end{bmatrix} \begin{bmatrix} 0 \\ -\omega_1\omega_3 \\ \omega_1\omega_2 \end{bmatrix} = \begin{bmatrix} 0 \\ -\omega_1\omega_3 \\ \omega_1\omega_2 \end{bmatrix} - \begin{bmatrix} 0 & 0 & 0 \\ 0 & 0 & 0 \\ c & 0 & 1 \end{bmatrix} \begin{bmatrix} 0 \\ -\omega_1\omega_3 \\ \omega_1\omega_2 \end{bmatrix} = \mathbf{0} \tag{20}$$

Consequently, equation (18) can be transformed into equation (21) .

$$\begin{aligned} \dot{\boldsymbol{e}} &= \boldsymbol{B}\boldsymbol{\omega} - \boldsymbol{F}\boldsymbol{C}\boldsymbol{B}\boldsymbol{\omega} - \boldsymbol{F}\boldsymbol{K}\boldsymbol{e} + \boldsymbol{F}\boldsymbol{C}\dot{\boldsymbol{\omega}}_d - \dot{\boldsymbol{\omega}}_d \\ &= (\boldsymbol{B} - \boldsymbol{F}\boldsymbol{C}\boldsymbol{B})(\boldsymbol{e} + \boldsymbol{\omega}_d) = \boldsymbol{F}\boldsymbol{K}\boldsymbol{e} + (\boldsymbol{F}\boldsymbol{C} - \boldsymbol{I}_{3\times3})\dot{\boldsymbol{\omega}}_d \\ &= (\boldsymbol{B} - \boldsymbol{F}\boldsymbol{C}\boldsymbol{B} - \boldsymbol{F}\boldsymbol{K})\boldsymbol{e} + (\boldsymbol{B} - \boldsymbol{F}\boldsymbol{C}\boldsymbol{B})\boldsymbol{\omega}_d + (\boldsymbol{F}\boldsymbol{C} - \boldsymbol{I}_{3\times3})\dot{\boldsymbol{\omega}}_d \end{aligned} \tag{21}$$

Because $\lim \boldsymbol{\omega}_d = \lim \dot{\boldsymbol{\omega}}_d = \mathbf{0}$, the angular velocity error system is Hurwitz stabilizable if and only if

$$\boldsymbol{P}(\boldsymbol{B} - \boldsymbol{F}\boldsymbol{C}\boldsymbol{B} - \boldsymbol{F}\boldsymbol{K}) + (\boldsymbol{B} - \boldsymbol{F}\boldsymbol{C}\boldsymbol{B} - \boldsymbol{F}\boldsymbol{K})^{\mathrm{T}}\boldsymbol{P} < \mathbf{0} \tag{22}$$

By choosing appropriate symmetric positive definite matrix $\boldsymbol{P}$, use YALMIP toolbox and we can obtain the unknown matrices $\boldsymbol{C}$ and $\boldsymbol{K}$.

Comparing the above two cases, it can be seen that the forms of the equivalent control term for Case 1 and Case 2 are the same; only the dimension of matrices $\boldsymbol{F}$, $\boldsymbol{C}$ and $\boldsymbol{K}$ is different.

Lemma 1: Adopt the reaching law

$$\dot{\boldsymbol{s}} = -k\boldsymbol{s} - \kappa \left|\boldsymbol{s}\right|^{\alpha} \operatorname{sgn}(\boldsymbol{s}), k > 0, \kappa > 0, 0 < \alpha < 1 \tag{23}$$

The error state $e(t)$ will reach the sliding surface in finite time, denoted by t^*:

$$t^* = \frac{1}{k(\alpha - 1)} \ln \frac{\kappa}{k\left|\boldsymbol{s}(0)\right|^{1-\alpha} + \kappa} \tag{24}$$

Proof: With equation (23) , we have

$$\boldsymbol{s}^{\mathrm{T}}\dot{\boldsymbol{s}} = -k\boldsymbol{s}^{\mathrm{T}}\boldsymbol{s} - \kappa\left|\boldsymbol{s}\right|^{\alpha}\boldsymbol{s}^{\mathrm{T}}\operatorname{sgn}(\boldsymbol{s}) = -k\left|\boldsymbol{s}\right|^{2} - \kappa\left|\boldsymbol{s}\right|^{\alpha-1}\boldsymbol{s}^{\mathrm{T}}(\left|\boldsymbol{s}\right|\operatorname{sgn}(\boldsymbol{s}))$$

$$= -(k + \kappa\left|\boldsymbol{s}\right|^{\alpha-1})\left|\boldsymbol{s}\right|^{2} = \frac{1}{2}\frac{d(\boldsymbol{s}^{\mathrm{T}}\boldsymbol{s})}{dt} = \frac{1}{2}\frac{d\left|\boldsymbol{s}\right|^{2}}{dt} = \left|\boldsymbol{s}\right|\frac{d\left|\boldsymbol{s}\right|}{dt}$$

Namely,

$$-(k + \kappa\left|\boldsymbol{s}\right|^{\alpha-1})\left|\boldsymbol{s}\right| = \frac{d\left|\boldsymbol{s}\right|}{dt}$$

Then,

$$dt = -\frac{d\left|\boldsymbol{s}\right|}{(k + \kappa\left|\boldsymbol{s}\right|^{\alpha-1})\left|\boldsymbol{s}\right|} = -\frac{\left|\boldsymbol{s}\right|^{-\alpha}d\left|\boldsymbol{s}\right|}{k\left|\boldsymbol{s}\right|^{1-\alpha} + \kappa} = \frac{1}{\alpha - 1}\frac{d\left|\boldsymbol{s}\right|^{1-\alpha}}{k\left|\boldsymbol{s}\right|^{1-\alpha} + \kappa}$$

Integrate the above equation and the reaching time can be obtained:

$$t^* = \frac{1}{\alpha - 1}\int_{|s(0)|}^{|s(t^*)|}\frac{d\left|\boldsymbol{s}\right|^{1-\alpha}}{k\left|\boldsymbol{s}\right|^{1-\alpha} + \kappa} = \frac{1}{k(\alpha - 1)}\ln(k\left|\boldsymbol{s}\right|^{1-\alpha} + \kappa)\Big|_{|s(0)|}^{|s(t^*)|} = \frac{1}{k(\alpha - 1)}\ln\frac{\kappa}{k\left|\boldsymbol{s}(0)\right|^{1-\alpha} + \kappa}$$

When $t \geq t^*, \boldsymbol{s} = 0, \dot{\boldsymbol{s}} = 0$, the conclusion is proved.

Theorem 1: Design sliding mode control law

$$\boldsymbol{u}^* = -\boldsymbol{C}\boldsymbol{B}\boldsymbol{\omega} - \boldsymbol{C}\boldsymbol{f}(\boldsymbol{\omega}) + \boldsymbol{C}\dot{\boldsymbol{\omega}}_d + \boldsymbol{K}\boldsymbol{\omega}_d - \boldsymbol{K}\boldsymbol{\omega} - k\boldsymbol{s} - \kappa\left|\boldsymbol{s}\right|^{\alpha}\operatorname{sgn}(\boldsymbol{s}) \tag{25}$$

Then, the error state starting from any initial point will reach the sliding surface in finite time. Consequently, the closed-loop system generated by equations (14) and (25) is globally asymptotically stable. To avoid chattering, sign function sgn($\boldsymbol{s}$) can be replaced by continuous function $\theta(s)$.

$$\theta(\boldsymbol{s}) = \frac{\boldsymbol{s}}{\left|\boldsymbol{s}\right| + \delta}$$

where δ is a very small positive constant.

Proof: Let a Lyapunov function candidate be of the form

$$V = \frac{1}{2}\boldsymbol{s}^2$$

The first derivative along the solutions of equation is

$$\begin{aligned}\boldsymbol{s}^{\mathrm{T}}\dot{\boldsymbol{s}} &= \boldsymbol{s}^{\mathrm{T}}\left[\boldsymbol{C}(\boldsymbol{B}\boldsymbol{\omega}+f(\boldsymbol{\omega})+\boldsymbol{F}\boldsymbol{u}^{*})-\boldsymbol{C}\dot{\boldsymbol{\omega}}_{d}+\boldsymbol{K}\boldsymbol{\omega}-\boldsymbol{K}\boldsymbol{\omega}_{d}\right]\\ &=\boldsymbol{s}^{\mathrm{T}}\left[\boldsymbol{C}\boldsymbol{B}\boldsymbol{\omega}+\boldsymbol{C}f(\boldsymbol{\omega})-\boldsymbol{C}\boldsymbol{B}\boldsymbol{\omega}-\boldsymbol{C}f(\boldsymbol{\omega})+\boldsymbol{C}\dot{\boldsymbol{\omega}}_{d}+\boldsymbol{K}\boldsymbol{\omega}_{d}-\boldsymbol{K}\boldsymbol{\omega}-k\boldsymbol{s}-\kappa|\boldsymbol{s}|^{\alpha}\operatorname{sgn}(\boldsymbol{s})-\boldsymbol{C}\dot{\boldsymbol{\omega}}_{d}+\boldsymbol{K}\boldsymbol{\omega}-\boldsymbol{K}\boldsymbol{\omega}_{d}\right]\\ &=\boldsymbol{s}^{\mathrm{T}}\left[-k\boldsymbol{s}-\kappa|\boldsymbol{s}|^{\alpha}\operatorname{sgn}(\boldsymbol{s})\right]\\ &=-k|\boldsymbol{s}|^{2}-\kappa|\boldsymbol{s}|^{\alpha+1}<0\end{aligned}$$

Therefore, the control law can ensure that the state reaches the switching surface in finite time. Once the state reaches the switching surface, it will be maintained on the switching surface. When the angular velocity error state is on the switching surface, the dynamics of the error system can be denoted by equation (21) . According to Theorem 1, the error system denoted by equation (21) is asymptotically stable. Therefore, the chaotic system denoted by equation (14) is asymptotically stable with controller (25), such that $\lim \boldsymbol{e}=\boldsymbol{0}$, and the proof is completed.

For $\lim \boldsymbol{\omega}_{d}=\boldsymbol{0}$, we have $\lim \boldsymbol{\omega}=\boldsymbol{0}$, so the chaotic system (9) and (10) are asymptotically stable with controller (25). To guarantee the limit of control input, we can choose the appropriate maximum boundary value $\boldsymbol{u}_{m}$, and the criterion for judgement is whether the boundary value will influence the system stability.

Simulation results

This section will test the effectiveness of the proposed controller by numerical simulations. Based on the spacecraft chaotic attitude motion of Chen system and Lu system, mathematical simulations are performed, respectively.

The moment of inertia of spacecraft in kilogram-square meter $\boldsymbol{I}=\operatorname{diag}(2,1,1)(\mathrm{kg}\cdot\mathrm{m}^{2})$, the reference angular velocity is given by $\boldsymbol{\omega}_{d}=\left[0.5\omega_{dr}\quad 0.6\omega_{dr}\quad \omega_{dr}\right]^{\mathrm{T}}$, the reference angular acceleration is given by $\dot{\boldsymbol{\omega}}_{d}=\left[0.5\dot{\omega}_{dr}\quad 0.6\dot{\omega}_{dr}\quad \dot{\omega}_{dr}\right]^{\mathrm{T}}$, the characteristic time instant is given by $t_{1}=15\mathrm{s}, t_{2}=40\mathrm{s}, t_{3}=60\mathrm{s}$, and the initial value of yaw angular velocity is given by $\omega_{dr0}=1.7189^{\circ}/\mathrm{s}$.

According to equation (13) , we have $\dot{\omega}_{m}=0.0364^{\circ}/\mathrm{s}^{2}$. Choose the maximum boundary value of control input $u_{m}=0.88$, the symmetric positive definite matrix $\boldsymbol{P}=\operatorname{diag}(0.01,0.02,0.03)$, and the related parameters of sliding mode controller $k=0.04, \kappa=0.01, \alpha=0.4$.

Case 1 (failure of one actuator): The initial value of angular velocity is chosen as $\boldsymbol{\omega}_{0}=[1.7189\quad 2.2918\quad 1.4324]^{\mathrm{T}\circ}/\mathrm{s}$, then, the solutions of equation (22) can be obtained using YALMIP toolbox, namely,

$$\boldsymbol{C}_{Chen}=\begin{bmatrix}0.2804 & 1 & 0\\ 0 & 0 & 1\end{bmatrix}, \boldsymbol{K}_{Chen}=\begin{bmatrix}27.3126 & 32.5001 & 0\\ 0 & 0 & 28.2085\end{bmatrix}$$

$$\boldsymbol{C}_{Lu}=\begin{bmatrix}0.2653 & 1 & 0\\ 0 & 0 & 1\end{bmatrix}, \boldsymbol{K}_{Lu}=\begin{bmatrix}27.5526 & 33.2601 & 0\\ 0 & 0 & 28.5418\end{bmatrix}$$

The simulation results for the Chen attitude chaotic system and Lu attitude chaotic system are shown in Figs.4-13. Fig.4 and Fig.5 display the time histories of the reference angular velocity and reference angular acceleration, which are in accordance with Fig.3. Fig.6 and Fig.7 display

the variations of angular velocity based on the Chen system and Lu system, respectively. Fig.8 and Fig.9 display the variations of angular velocity error based on the Chen system and Lu system, respectively. As can be seen, the convergence time is 60s, which is the same with the characteristic time instant t_3. These four figures indicate that the angular velocity and angular velocity error could rapidly converge in the presence of external disturbances, which lead to a chaotic motion.

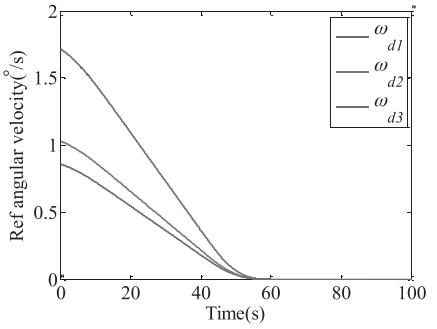

Figure 4. Reference angular velocity.

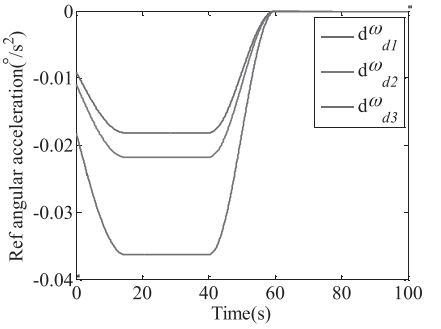

Figure 5. Reference angular acceleration.

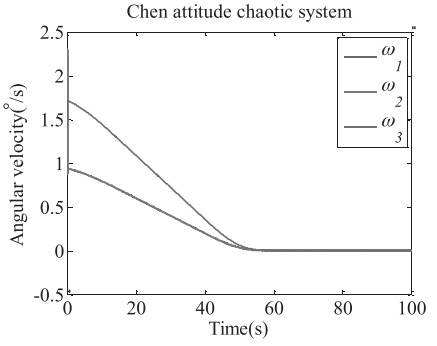

Figure 6. Angular velocity based on the Chen system in Case 1.

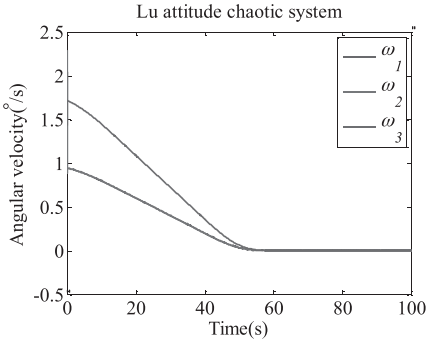

Figure 7. Angular velocity based on the Lu system in Case 1.

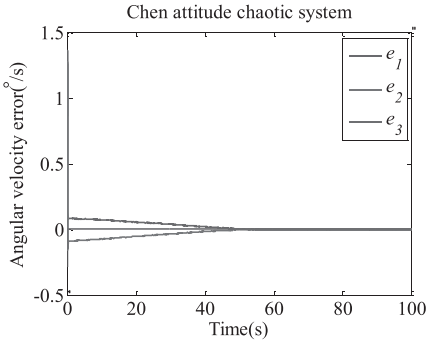

Figure 8. Angular velocity error based on the Chen systemin Case 1.

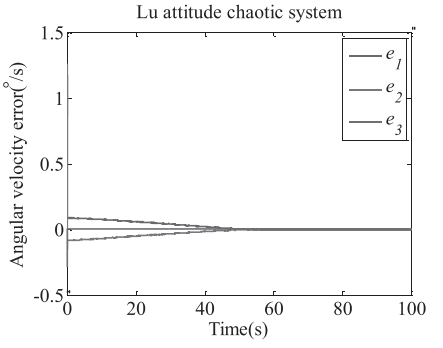

Figure 9. Angular velocity error based on the Lu systemin Case 1.

Fig.10 and Fig.11 display the variations of control torque, and the value satisfies the given restraint condition. Fig.12 and Fig.13 display the external disturbance torque curves imposed on the spacecraft that lead to a chaotic attitude motion. These four figures indicate that the control torque

and external disturbance torque both rapidly converge to zero, and the control torque and the external disturbance torque are approximately equal but in opposite directions.

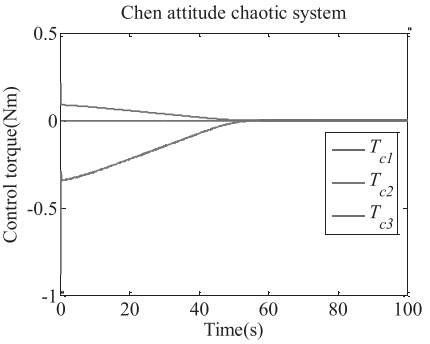

Figure 10. Control torque based on the Chen system in Case 1.

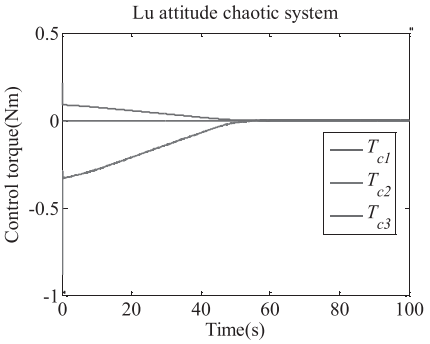

Figure 11. Control torque based on the Lu system in Case 1.

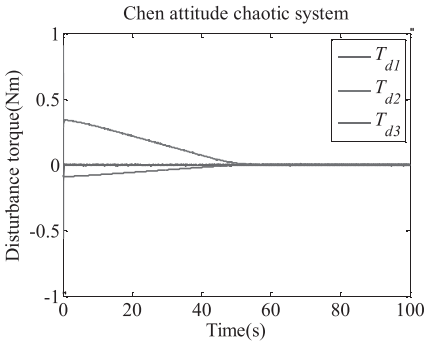

Figure 12. Disturbance torque based on the Chen system in Case 1.

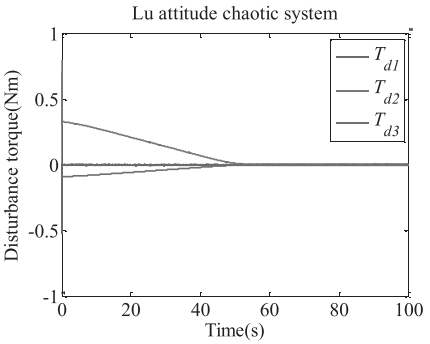

Figure 13. Disturbance torque based on the Lu system in Case 1.

Case 2 (failures of two actuators): When the initial value of the angular velocity is chosen as $\boldsymbol{\omega}_0 = [0 \quad 0 \quad 1.4324]^{\mathrm{T}\circ}$/s, then, the solutions of equation (22) can be obtained using YALMIP toolbox, namely,

$$\boldsymbol{C}_{Chen} = \begin{bmatrix} 0 & 0 & 1 \end{bmatrix}, \boldsymbol{K}_{Chen} = \begin{bmatrix} 0 & 0 & 3.9892 \end{bmatrix}$$
$$\boldsymbol{C}_{Lu} = \begin{bmatrix} 0 & 0 & 1 \end{bmatrix}, \boldsymbol{K}_{Lu} = \begin{bmatrix} 0 & 0 & 6.3468 \end{bmatrix}$$

The simulation results for the Chen attitude chaotic system and Lu attitude chaotic system are shown in Figs.14–21. Fig.14 and Fig.15 display the time histories of the angular velocity based on the Chen system and Lu system, respectively. Fig.16 and Fig.17 display the variations of angular velocity error based on the Chen system and Lu system, respectively. As can be seen, the convergence time is 60s, which is the same with the characteristic time instant t_3. These four figures indicate that the angular velocity and angular velocity error could rapidly converge in the presence of external disturbances, which lead to a chaotic motion.

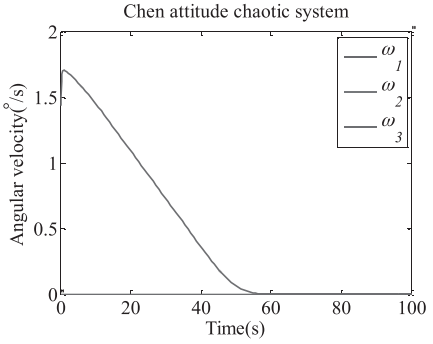

Figure 14. Angular velocity based on the Chen system in Case 2.

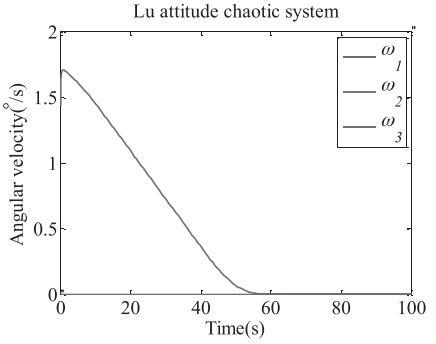

Figure 15. Angular velocity based on the Lu system in Case 2.

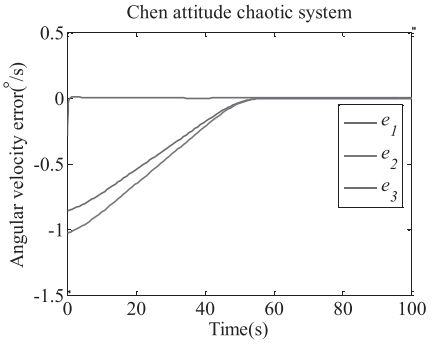

Figure 16. Angular velocity error based on the Chen system in Case 2.

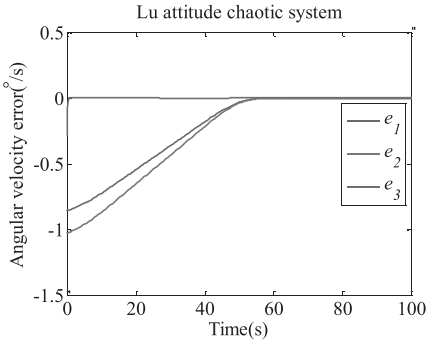

Figure 17. Angular velocity error based on the Lu system in Case 2.

Fig.18 and Fig.19 display the variations of control torque, and the value satisfies the given restraint condition. Fig.20 and Fig.21 display the external disturbance torque curves imposed on the spacecraft that leads to a chaotic attitude motion. These four figures indicate that the control torque and external disturbance torque both rapidly converge to zero, and they are much smaller than those corresponding to Case 1.

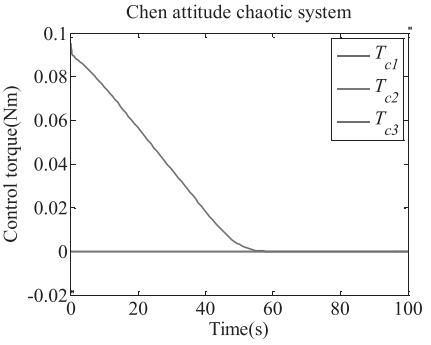

Figure 18. Control torque based on the Chen system in Case 2.

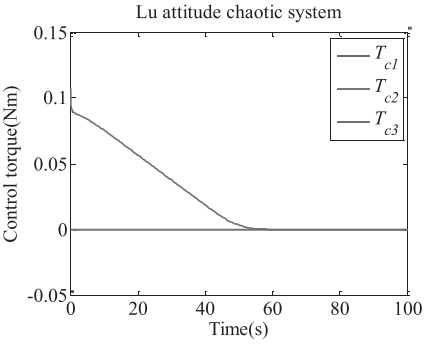

Figure 19. Control torque based on the Lu system in Case 2.

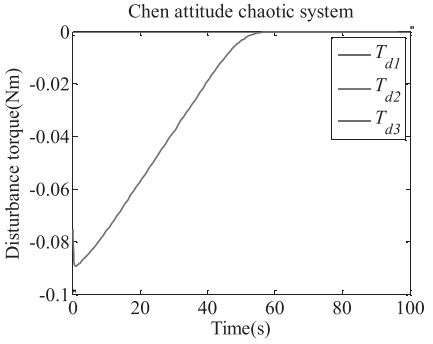

Figure 20. Disturbance torque based on the Chen system in Case 2.

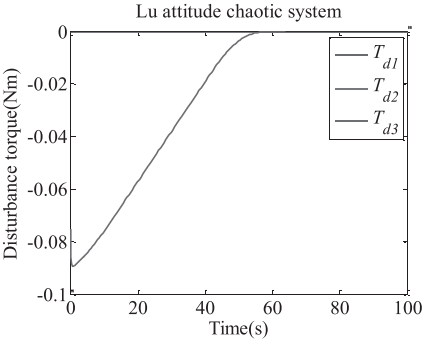

Figure 21. Disturbance torque based on the Lu system in Case 2.

If one of the initial angular velocities along the x-axis or y-axis is not strictly zero, there is a very small perturbation. For example, $\boldsymbol{\omega}_0 = [5.73\times10^{-7} \quad 0 \quad 1.4324]^{\mathrm{T}\circ}/\mathrm{s}$, the variations of the angular velocity based on the Chen system and Lu system can be seen in Fig.22 and Fig.23, respectively. This indicates that the spacecraft attitude motion is still chaotic, and the designed controller becomes invalid. This is in accordance with the prerequisite of controller design.

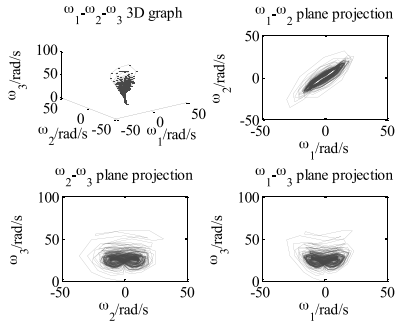

Figure 22. ω1-ω2-ω3 3D graph and its projection based on the Chen system.

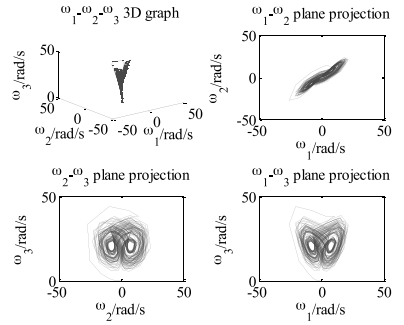

Figure 23. ω1-ω2-ω3 3D graph and its projection based on the Lu system.

CONCLUSIONS

A novel sliding mode control method with control input constraint has been proposed in this paper. To deal with certain actuator failure and chaotic motion problem of spacecraft attitude system, integral sliding mode and angular velocity tracking ideas are incorporated into the controller, which consists of equivalent control term and switching control term. A detailed stability proof of the closed-loop system is also included based on Lyapunov analysis. When the failure of one actuator occurs, the angular velocities along three principal axes can be stabilized. Under given conditions, the spacecraft chaotic attitude system will be controllable when the failures of two actuators occur. Moreover, simulations are performed to assess the effectiveness and feasibility. The simulation results indicate that the controller presented in this paper has the following characteristics: (a) elimination of chaotic attitude motion, (b) explicit consideration of control input constraint, (c) presupposition of attitude stabilization time, (d) track reference angular velocity trajectory designed in advance, (e) consideration of certain actuator failure, and (f) robustness to bigger

external disturbance torque. Therefore, the proposed sliding mode controller can be applied in practical stabilization control of spacecraft chaotic attitude motion under control input constraint.

REFERENCES

Aeyels, D. 1985. Stabilization by smooth feedback of the angular velocity of a rigid body. Systems & control letters, **6**(1), 59-63.

Aeyels, D. & Szafranski, M. 1988. Comments on the stabilizability of the angular velocity of a rigid body. Systems & Control Letters, **10**(1), 35-39.

Aghababa, M. P. & Aghababa, H. P. 2013. Robust synchronization of a chaotic mechanical system with nonlinearities in control inputs. Nonlinear Dynamics, **73**(1-2), 363-376.

Alwi, H. & Edwards, C. 2008. Fault tolerant control using sliding modes with on-line control allocation. Automatica, **44**(7), 1859-1866.

Alwi, H., Edwards, C., Stroosma, O. & Mulder, J. A. 2008. Fault tolerant sliding mode control design with piloted simulator evaluation. Journal of Guidance, Control, and Dynamics, **31**(5), 1186-1201.

Beletsky, V. V., Lopes, R. V. F. & Pivovarov, M. L. 1999. Chaos in spacecraft attitude motion in Earth's magnetic field. Chaos: An Interdisciplinary Journal of Nonlinear Science, **9**(2), 493-498.

Bloch, A. M. & Marsden, J. E. 1990. Stabilization of rigid body dynamics by the energy-Casimir method. Systems & Control Letters, **14**(4), 341-346.

Brockett, R. W. 1983. Asymptotic stability and feedback stabilization. Differential geometric control theory, **27**(1), 181-191.

Crouch, P 1984. Spacecraft attitude control and stabilization: Applications of geometric control theory to rigid body models. IEEE Transactions on Automatic Control, **29**(4), 321-331.

Hu, Q. 2010. Robust adaptive sliding-mode fault-tolerant control with L2-gain performance for flexible spacecraft using redundant reaction wheels. IET Control Theory & Applications, **4**(6), 1055-1070.

Ke, Z., Zhi-Hui, W., Li-Ke, G., Yue, S. & Tie-Dong, M. 2015. Robust sliding mode control for fractional-order chaotic economical system with parameter uncertainty and external disturbance. Chinese Physics B, **24**(3), 030504.

Kerai, E. 1995. Analysis of small time local controllability of the rigid body model. Proceedings of the IFAC symposium on system structure and control, 645-650.

Kuntanapreeda, S. 2009. Chaos synchronization of unified chaotic systems via LMI. Physics Letters A, **373**(32), 2837-2840.

Liao, F., Wang, J. L. & Yang, G. H. 2002. Reliable robust flight tracking control: an LMI approach. IEEE Transactions on Control Systems Technology, **10**(1), 76-89.

Lu, J. G. 2006. Chaotic dynamics of the fractional-order lü system and its synchronization. Physics Letters A, **59**(4), 305-311.

Lu, J. G. & Chen, G. 2006. A note on the fractional-order chen system. Chaos Solitons & Fractals, **27**(3), 685-688.

Luo, W., Chu, Y. C. & Ling, K. V. 2005. H∞ inverse optimal attitude-tracking control of rigid spacecraft. Journal of guidance, control, and dynamics, **28**(3), 481-494.

Ma, Y., Jiang, B., Tao, G. & Cheng, Y. 2015. Uncertainty decomposition-based fault-tolerant adaptive control of flexible spacecraft. IEEE Transactions on Aerospace and Electronic Systems, **51**(2), 1053-1068.

Meehan, P. A. & Asokanthan, S. F. 2002. Control of chaotic instabilities in a spinning spacecraft with dissipation using Lyapunov›s method. Chaos, Solitons & Fractals, **13**(9), 1857-1869.

Rubagotti, M., Estrada, A., Castanos, F., Ferrara, A. & Fridman, L. 2011. Integral sliding mode control for nonlinear systems with matched and unmatched perturbations. IEEE Transactions on Automatic Control, **56**(11), 2699-2704.

Shen, Q., Wang, D., Zhu, S. & Poh, E. K. 2015. Integral-type sliding mode fault-tolerant control for attitude stabilization of spacecraft. IEEE Transactions on Control Systems Technology, **23**(3), 1131-1138.

Utkin, V., Guldner, J. & Shi, J. 2009. Sliding mode control in electro-mechanical systems, **34**. CRC press.

Utkin, V. & Shi, J. 1996. Integral sliding mode in systems operating under uncertainty conditions. Proceedings of the 35th IEEE Conference on Decision and Control, **4**, 4591-4596.

Wang, Z. & Wu, Z. 2015. Nonlinear attitude control scheme with disturbance observer for flexible spacecrafts. Nonlinear Dynamics, **81**(1-2), 257-264.

Wei, W. 2015. Synchronization of coupled chaotic Hindmarsh Rose neurons: An adaptive approach. Chinese Physics B, **24**(10), 100503.

Xiao, B., Hu, Q. & Zhang, Y. 2012. Adaptive sliding mode fault tolerant attitude tracking control for flexible spacecraft under actuator saturation. IEEE Transactions on Control Systems Technology, **20**(6), 1605-1612.

Yang G. H., Wang J. L. & Soh Y. C. 2001. Reliable H∞, controller design for linear systems. Automatica, **37**(5): 717-725.

Yau, H. T. & Shieh, C. S. 2008. Chaos synchronization using fuzzy logic controller. Nonlinear analysis: Real world applications, **9**(4), 1800-1810.

Zhang, Y. & Jiang, J. 2008. Bibliographical review on reconfigurable fault-tolerant control systems. Annual reviews in control, **32**(2), 229-252.

Zhang, R., Qiao, J., Li, T. & Guo, L. 2014. Robust fault-tolerant control for flexible spacecraft against partial actuator failures. Nonlinear Dynamics, **76**(3), 1753-1760.

Zolghadri, A. 2012. Advanced model-based FDIR techniques for aerospace systems: Today challenges and opportunities. Progress in Aerospace Sciences, **53**, 18-29.

Submitted: 12/06/2016
Revised : 05/12/2016
Accepted : 20/02/2017